

Equations for solar tracking

A. Merlaud

Belgian Institute for Space Aeronomy(IASB-BIRA), Brussels

January 12, 2013

Abstract

Direct Sun light absorption by trace gases can be used to quantify them and investigate atmospheric chemistry. In such experiments, the main optical apparatus is often a grating or a Fourier transform spectrometer. A solar tracker based on motorized rotating mirrors is also needed to direct the light along the spectrometer axis, correcting for the apparent rotation of the Sun. Calculating the Sun azimuth and altitude for a given time and location can be achieved with high accuracy but different sources of angular offsets appear in practice when positioning the mirrors. A feedback on the motors, using a light position sensor closed to the spectrometer is almost always needed. This paper aims to gather the main geometrical formulas necessary for the use of a widely used kind of solar tracker, based on two 45° mirrors in altazimuthal set-up with a light sensor on the spectrometer, and to illustrate them with a tracker developed for atmospheric research by our group.

1 Introduction

Spectroscopic studies of direct Sun light are commonly used in atmospheric research. Such experiments make use of the Sun as a light source to quantify molecular absorptions in the atmosphere and then retrieve trace gases abundance. Stratospheric ozone [1] and greenhouse gases [2] are routinely measured with this technique from ground-based Fourier transform infrared(FTIR) spectrometers, e.g. within the Network for the Detection of Atmospheric Composition Change (NDACC, <http://www.ndacc.org/>). In the UV-visible range, light scattering is more important and enables spectroscopic studies of the atmosphere in other geometries such as zenith measurements [3]. Direct sun light is however also used [4, 5], its unique and unambiguous light path making it advantageous for some applications [6]. Beside the spectrometer, the main part of the involved apparatus in direct sun light spectroscopy is the solar tracker, required to compensate for the Sun's apparent movement.

Several kinds of trackers, sometimes referred as heliostats, are used for atmospheric spectroscopy, based on set-ups of one or several rotating mirrors. Some of them are equatorially mounted, like in Table Mountain Facility [4] or Harestua [7]. In this case, one rotational axis is parallel to the Earth's axis. It enables a high tracking accuracy without a computer, since only one axis has to be driven at the Earth's rotation speed. To our knowledge, it is the only set-up working without retroaction on the Sun's position. On the other hand, equatorial mounts are large, need to be aligned accurately and their mechanical design is difficult. Most of the trackers used today are controlled by a computer which makes possible remote operation and automatization. The computer calculates first the Sun position, moves the mirrors to point the Sun and then controls this mirror to optimize the signal on some kind of light sensor.

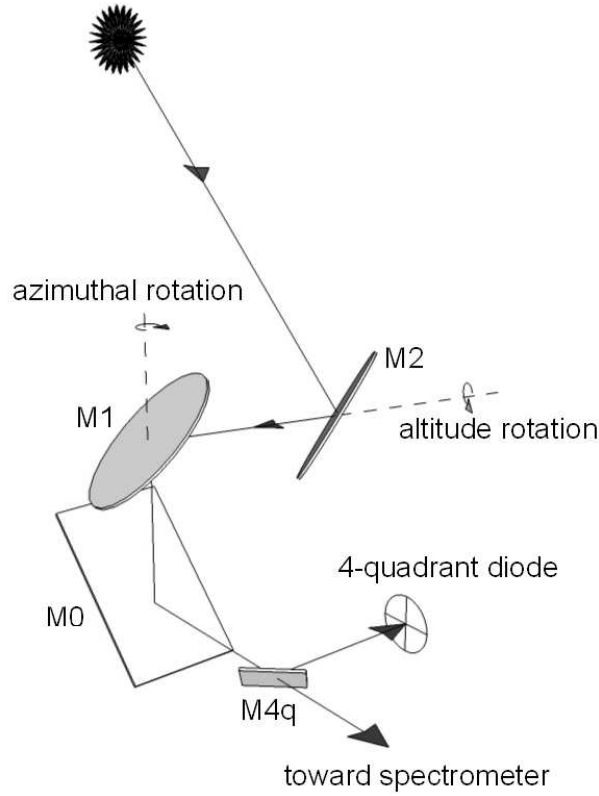


Figure 1: Geometrical set-up of the considered solar tracker, using two 45-degree mirrors, M1 and M2, rotating along orthogonal axes. Mirror M0 directs the Sun light into a spectrometer. A fraction of the light beam is deflected toward a 4-quadrant photodiode enabling a closed-loop control of the mirrors position.

Figure 1 shows a popular altazimuthal tracker design. It consists of two elliptical mirrors held in 45 degrees facing each other (M1 and M2). Both M1 and M2 rotate along the azimuthal axis and M2 rotates as well along the altitude direction. M0, and possibly other fixed mirrors, sets the light beam into the spectrometer optical axis. A 4-quadrant photodiode is used as a position sensor for a closed-loop control of the mirrors position once the Sun's calculated position has been reached with enough accuracy, i.e. once the Sun's image is visible by the photodiode. This altazimuthal set-up is used with FTIR systems e.g. in Kiruna [8] and Park Falls, Wisconsin [9], it has been installed in Harestua to replace the equatorially mounted system [10]. Compact versions have also been developed for field campaigns [11, 12]. A commercial version is sold by Bruker to be installed above their FTIR spectrometers [13]. A recent progress has been reported in the pointing accuracy [14], replacing the traditional quadrant diode with a CCD camera, but the problems discussed thereafter remain the same.

Because developing a solar tracker is typically a master's thesis work [8, 12, 11], technical implementations are difficult to access in the literature. Some more information is available about the systems used in solar energy applications but their geometry differ [15, 16]. Someone building a Sun tracker can quickly find ephemeris calculations in many programming languages, but other issues arise quickly. It is first necessary to characterize the field-of-view(FOV) of the 4-quadrant diode in the considered optical design. This serves two purposes: determining the accuracy needed for the ephemeris's algorithm and making sure this FOV is larger than the Sun's apparent diameter(9 mrad). This last point is important to track constantly the center of the Sun, which reduces the uncertainties in the air mass factor and avoid Doppler shifts on the edges of the Sun ([14]). A second problem lies in the correction of the tracker orientation compared to the altazimuthal system in which the ephemeris is given, necessary for the calculated mode if the ground is not leveled. Thirdly, the relation between the quadrant signal and the correction to apply on the mirrors position depends on the tracker position itself [14]. Understanding this relation is compulsory to achieve a smooth tracking. This article deals with these three problems successively.

2 Theoretical basis

2.1 Ephemeris accuracy and field of view of the 4-quadrant diode

Calculating the Sun position in the sky given the time of observation and the geographical coordinates is well documented. A reference algorithm with a typical error as low as 0.0003° is given by Jean Meeus in [17], for which C([18]) or Matlab ([19]) versions are available. This accuracy degrades with higher zenithal angle due to atmospheric refraction, which depends on local

meteorological conditions [20]. On the other hand, the absolute accuracy of commercial rotation stages used in Sun trackers, e.g Newport RV-160, is only 0.01° , which reduces the interest of using a complex algorithm. The lowest acceptable accuracy is determined by the field of view of the 4-quadrant diode: once the Sun image hits the quadrant, the tracking can be performed in closed-loop.

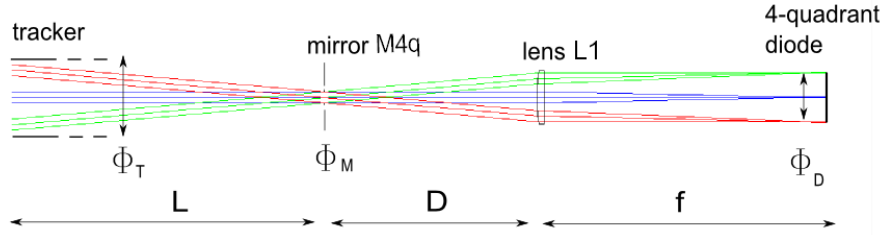


Figure 2: Optical scheme from the tracker mirrors to the 4-quadrant diode. The field of view seen by the diode depends on the different aperture sizes and path lengths.

Figure 2 shows the typical optical scheme between the tracker and the quadrant diode, the optical axis has been aligned for the sake of clarity. Close to the spectrometer, a part of the beam from the tracker, whose diameter is limited by the mirror diameter Φ_T is deflected by a mirror of diameter Φ_M to a lens which focuses the beam onto the quadrant. The maximum field-of-view seen by the diode (FOV_1) depends on the focal length of the lens (f) and on the diameter of the quadrant (Φ_D), according to $FOV_1 = \arctan \frac{\Phi_D}{f}$. The lens L1 is unlikely to reduce the FOV assuming its size superior to the mirror's one. Indeed, the beam is parallel before the lens which implies that distance D can be reduced if necessary. The tracker aperture is more important, especially since the diameter of rotation stage is limited and the distance between the tracker and the deflecting mirror (M4) depends on the observatory configuration. The mirror's FOV due to the tracker is $FOV_2 = \arctan \frac{\Phi_T}{L}$.

Considering our set-up in Brussels, which is a typical FTIR station, the tracker's mirrors are 10 cm wide and the optical path to the spectrometer 5m long, which leads to a FOV_2 of 20 mrad. On the other hand, the quadrant diameter is 6 mm while the focal length of the lens is 200mm, which gives 30 mrad for FOV_1 . The actual FOV is the minimum, 20 mrad, limited by the tracker size. This value is superior to the apparent diameter of the Solar disk which is important to track the center of the Sun. A simple algorithm can achieve such an accuracy for the ephemeris calculation, like the one given by NOAA([21]). It is however necessary to take into account the orientation

of the tracker, which can lead to pointing errors superior to the FOV.

2.2 Correcting the tracker orientation

A source of error when pointing to the calculated Sun position originate from the orientation of the observatory compared to the altazimuthal system. If the ground is not completely leveled, this problem add offsets to the calculated positions, which are not constant during the day. To take that into account in the calculation requires to determine the Euler Angles of the observatory frame compared to the altazimuthal system. We discuss their effects before describing our way to determine them.

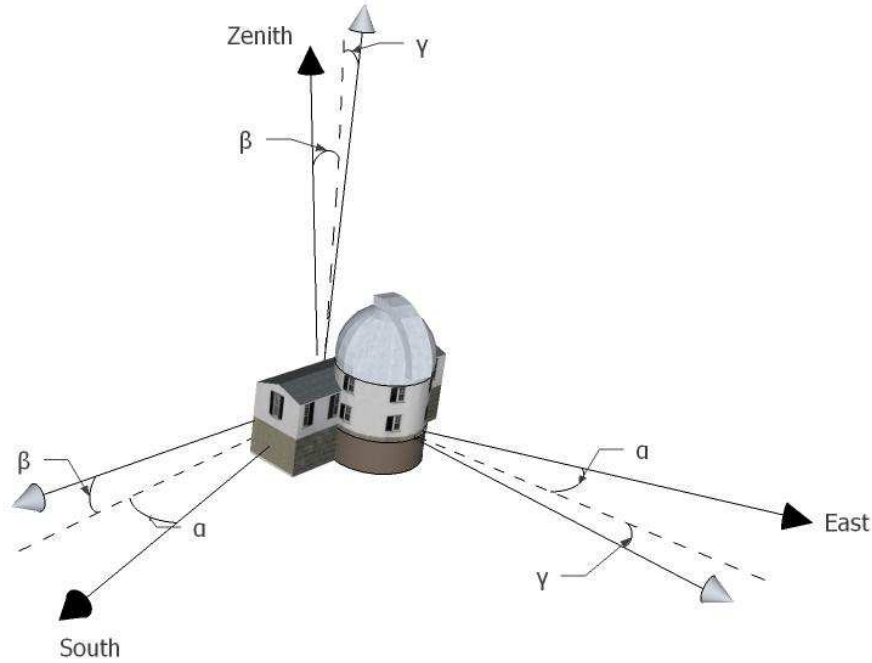


Figure 3: Illustration of the Euler Angles of an observatory compared to the altazimuthal coordinates system.

Euler angles represents the consecutive rotation on the three axes needed to account for the pitch(γ), roll(β) and yaw(α) of the observatory. Converting the solar altitude and azimuth to the observatory frame requires thus to compute the multiplication of three rotation matrices along the different axes, i.e $R_x(\gamma)$, $R_y(\beta)$ and $R_z(\alpha)$.

$$M_{offsets} = \begin{bmatrix} 1 & 0 & 0 \\ 0 & \cos \gamma & -\sin \gamma \\ 0 & \sin \gamma & \cos \gamma \end{bmatrix} \times \begin{bmatrix} \cos \beta & 0 & \sin \beta \\ 0 & 1 & 0 \\ -\sin \beta & 0 & \cos \beta \end{bmatrix} \times \begin{bmatrix} \cos \alpha & -\sin \alpha & 0 \\ \sin \alpha & \cos \alpha & 0 \\ 0 & 0 & 1 \end{bmatrix} \quad (1)$$

The calculations leads to:

$$M_{offsets} = \begin{bmatrix} \cos \alpha \cos \beta & -\sin \alpha \cos \beta & \sin \beta \\ \cos \alpha \sin \beta \sin \gamma + \sin \alpha \cos(\gamma) & \cos \alpha \cos \gamma - \sin \alpha \sin \beta \sin \gamma & -\cos \beta \sin \gamma \\ \sin \alpha \sin \gamma - \cos \alpha \sin \beta \cos \gamma & \cos \alpha \sin \gamma + \sin \alpha \sin \beta \cos \gamma & \cos \beta \cos \gamma \end{bmatrix} \quad (2)$$

In Cartesian coordinates, the position of the Sun(x_t, y_t, z_t) in the observatory frame will thus be related to the solar spherical coordinates(az_0, alt_0) in the altazimuthal system:

$$\begin{bmatrix} x_t \\ y_t \\ z_t \end{bmatrix} = M_{offsets} \times \begin{bmatrix} \cos alt_0 \cos az_0 \\ \cos alt_0 \sin az_0 \\ \sin alt_0 \end{bmatrix} \quad (3)$$

In the above equation, the distance from the observatory to the Sun, r , is set to unity. This does not matter for the application and simplifies the calculation. Substituting M_{offset} with Eq. 2 we get the following expressions for those coordinates:

$$\begin{cases} x_t = (\cos \alpha \cos alt_0 \cos az_0 - \sin \alpha \cos alt_0 \sin az_0) \cos \beta \\ \quad + \sin alt_0 \sin \beta \\ y_t = (\cos \alpha \cos alt_0 \sin az_0 + \sin \alpha \cos alt_0 \cos az_0) \cos \gamma \\ \quad - (\cos \alpha \cos alt_0 \cos az_0 - \sin \alpha \cos alt_0 \sin az_0) \sin \beta \sin \gamma \\ \quad - \sin alt_0 \cos \beta \sin \gamma \\ z_t = (\cos \alpha \cos alt_0 \sin az_0 + \sin \alpha \cos alt_0 \cos az_0) \sin \gamma \\ \quad - (\cos \alpha \cos alt_0 \cos az_0 - \sin \alpha \cos alt_0 \sin az_0) \sin \beta \cos \gamma \\ \quad + \sin alt_0 \cos \beta \cos \gamma \end{cases} \quad (4)$$

These new Cartesian coordinates can then be converted to altitude(alt_t) and azimuth(az_t) angles relative to the tracker:

$$\begin{cases} \rho_t &= \sqrt{x_t^2 + y_t^2} \\ alt_t &= \arctan_{4q} \frac{z_t}{\rho_t} \\ az_t &= \arctan_{4q} \frac{y_t}{x_t} \end{cases} \quad (5)$$

In the above equation \arctan_{4q} stands for the variation of the arctangent function called *atan2* in many programming languages.

Determining Euler angles accurately by measurements is not easy. An analytical method to estimate them is given in [15] which basically consists in recording the position of the tracker at three different times and solving Eq. 4. This is appropriate for the studied case, i.e. a collector for solar energy application installed outside with only one mirror and no closed-loop control. With our considered two-mirror tracker, which does not collect light but directs it toward a spectrometer, other source of misalignments appear. Indeed, the tracker is also likely to be misaligned compared to the spectrometer, and mirror themselves can be tilted. Other angles can be considered in $M_{offsets}$ and is done in [8]. However as some of them change with time (due to thermal expansion for instance), it is not very useful. In practical applications the three offsets are likely to enable the calculated mode to reach the Sun within the FOV of the 4-quadrant diode. With the closed-loop control it is easy to track the Sun a whole clear-sky day providing an operator correctly sets the Sun tracker initially. Euler angles can then be fitted all along the recorded positions of the mirrors during the day. It has the advantage that other sources of misalignment are considered; even if only three angles are fitted which may not exactly be the Euler angles, they minimize simultaneously the effects of all offsets. We implement this method in Sect. 3. This requires the closed-loop control of the tracker on the Sun position.

2.3 Active tracking

The photodiode signal indicates how tilted the Sun beam is compared to the optical axis of the spectrometer. This information must be converted into angular displacements on the altitude and azimuth axes of the tracker to correct the misalignment. If the photodiode was placed on the reference frame of the mirror M2 this conversion would be straightforward, but due to its position after the tracker it depends on the position of the tracker mirrors. A try-and-error method to correct the misalignment is theoretically possible but a smoother tracking can be achieved if the conversion is understood.

The conversion can be expressed once again by a matrix, which transform in this case a vector hitting mirror M1 to a vector pointing to a direction in the sky given by its altitude and azimuth. It is the opposite of the light direction but is simpler to figure out and considering Fermat principle, yields the same information.

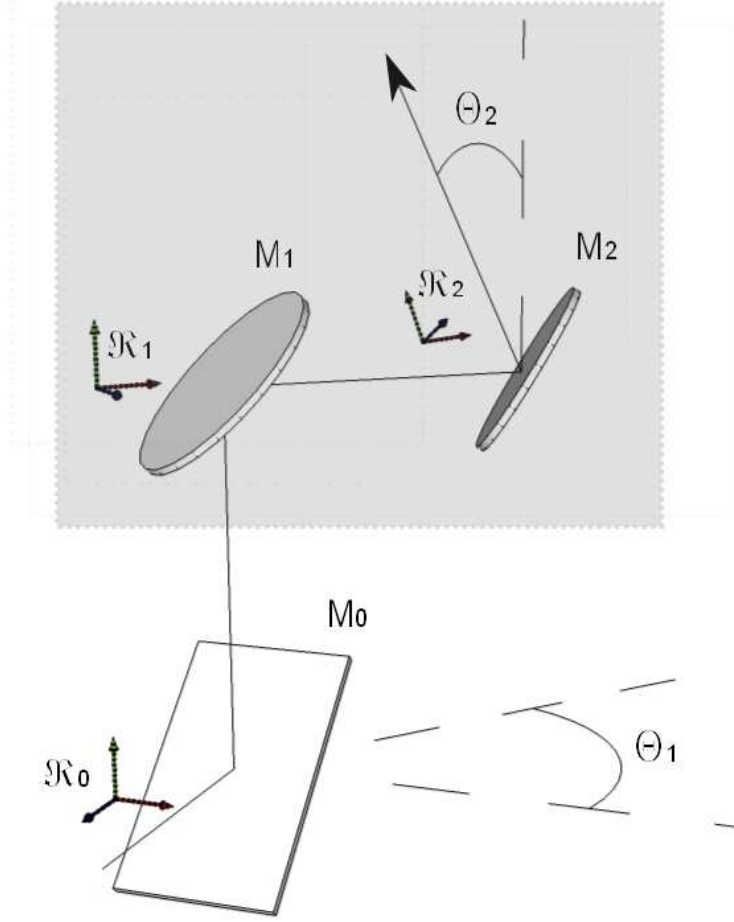


Figure 4: The tracker mirrors and their rotation can be modeled as rotation matrices in their reference frames, which apply to the beam vector.

As with the Euler Angles, the transformation reduces conveniently to a combination of rotation matrices. For instance, compared to the reference frame \mathcal{R}_0 , the reflection on mirror M_0 is expressed as $R_y(\pi/2)$ while the azimuthal rotation of an angle θ_1 is written $R_z(\theta_1)$.

Figure 4 presents the tracker pointing to an azimuth θ_1 and a zenith angle of θ_2 . The optical system inside the frame, with only mirrors M_1 and M_2 can be expressed as a transformation whose matrix $M_{tracker}$ is:

$$M_{tracker} =$$

$$R_z(\theta_1) \times R_y(\theta_2) \times R_x\left(\frac{\pi}{2}\right) \times R_y(-\theta_2) \times R_x\left(-\frac{\pi}{2}\right) \times R_z(-\theta_1) \quad (6)$$

i.e:

$$M_{tracker} =$$

$$\begin{bmatrix} \cos \theta_1 & -\sin \theta_1 & 0 \\ \sin \theta_1 & \cos \theta_1 & 0 \\ 0 & 0 & 1 \end{bmatrix} \times \begin{bmatrix} \cos \theta_2 & 0 & \sin \theta_2 \\ 0 & 1 & 0 \\ -\sin \theta_2 & 0 & \cos \theta_2 \end{bmatrix} \times \begin{bmatrix} 1 & 0 & 0 \\ 0 & 0 & -1 \\ 0 & 1 & 0 \end{bmatrix} \times \\ \begin{bmatrix} \cos \theta_2 & 0 & -\sin \theta_2 \\ 0 & 1 & 0 \\ \sin \theta_2 & 0 & \cos \theta_2 \end{bmatrix} \times \begin{bmatrix} 1 & 0 & 0 \\ 0 & 0 & 1 \\ 0 & -1 & 0 \end{bmatrix} \times \begin{bmatrix} \cos \theta_1 & \sin \theta_1 & 0 \\ -\sin \theta_1 & \cos \theta_1 & 0 \\ 0 & 0 & 1 \end{bmatrix} \quad (7)$$

Developing the matrix product yields to the matrix of the tracker optical system as a function of the tracker position (θ_1, θ_2) :

$$M_{tracker} =$$

$$\begin{bmatrix} \cos \theta_1 \cos \theta_2 \cos(\theta_1 + \theta_2) + \sin \theta_1 \sin(\theta_1 + \theta_2) & \cos \theta_1 \cos \theta_2 \sin(\theta_1 + \theta_2) - \sin \theta_1 \cos(\theta_1 + \theta_2) & \cos \theta_1 \sin \theta_2 \\ \sin \theta_1 \cos \theta_2 \cos(\theta_1 + \theta_2) - \cos \theta_1 \sin(\theta_1 + \theta_2) & \cos \theta_1 \cos(\theta_1 + \theta_2) + \sin \theta_1 \cos \theta_2 \sin(\theta_1 + \theta_2) & \sin \theta_1 \sin \theta_2 \\ -\sin \theta_2 \cos \theta_1 + \theta_2 & -\sin \theta_2 \sin \theta_1 + \theta_2 & \cos \theta_2 \end{bmatrix}$$

The transformation expressed by $M_{tracker}$ can now be applied to a vector corresponding to the Sun light beam direction on the spectrometer side of the tracker, it will lead to the position of the Sun in Cartesian coordinates. The vector is built from the diode 4 signals (VA,VB,VC,VD), as represented in Fig. 5. Basically an offset position $(\varepsilon_1, \varepsilon_2)$ is computed for the Sun spot on the diode plane compared to its center by:

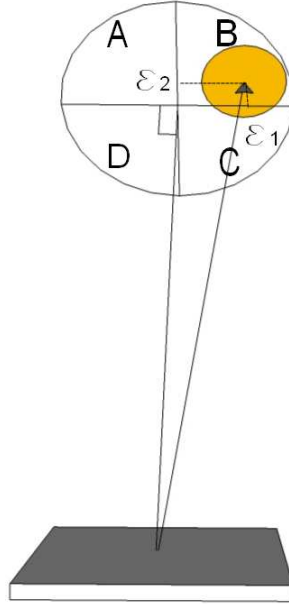


Figure 5: Sun spot hitting the quadrant, not to scale.

$$\begin{cases} \varepsilon_1 = (V_B + V_C) - (V_A + V_D) \\ \varepsilon_2 = (V_A + V_B) - (V_C + V_D) \end{cases} \quad (8)$$

The spot offset $(\varepsilon_1, \varepsilon_2)$ defines 2 coordinates of the beam vector. The last one, Λ , should represent the distance from the diode to mirror M1. Multiplying $M_{tracker}$ by the quadrant vector $(\varepsilon_1, \varepsilon_2, \Lambda)$ would yield accurate Sun angles after conversion to spherical coordinates, but is not practically possible with a diode, contrary to an imaging sensor. The calculated position (x_s, y_s, z_s) hereafter is thus not absolute but is sufficient to get the sign of the rotations to apply on the axes. Λ can be chosen arbitrarily as long as its absolute value is large enough compared to ε_1 and ε_2 . The solar pseudo-coordinates are then:

$$\begin{bmatrix} x_s \\ y_s \\ z_s \end{bmatrix} = M_{tracker} \times \begin{bmatrix} \varepsilon_1 \\ \varepsilon_2 \\ \Lambda \end{bmatrix} \quad (9)$$

In practice, the quadrant vector may differ from $(\varepsilon_1, \varepsilon_2, \Lambda)$ due to reflections such as on the mirrors M0 and M4q on Fig. 1, necessary to deviate a part of the beam to the 4-quadrant photodiode. Defining the position vector requires thus to pay attention on the optic path from M1 to the photodiode, but this is rather easy and reduce to a rotation once the image of the photodiode under M1 is figured out. In the next section, we explain how we deal with the problem in our particular case.

Developing Eq. 9 yields to:

$$\begin{cases} x_s = (\cos \theta_1 \cos \theta_2 \sin (\theta_1 + \theta_2) - \sin \theta_1 \cos (\theta_1 + \theta_2))\varepsilon_2 \\ \quad + (\sin \theta_1 \sin (\theta_1 + \theta_2) + \cos \theta_1 \cos \theta_2 \cos (\theta_1 + \theta_2))\varepsilon_1 \\ \quad + \Lambda \cos \theta_1 \sin \theta_2 \\ y_s = (\sin \theta_1 \cos \theta_2 \sin (\theta_1 + \theta_2) + \cos \theta_1 \cos (\theta_1 + \theta_2))\varepsilon_2 \\ \quad + (\sin \theta_1 \cos \theta_2 \cos (\theta_1 + \theta_2) - \cos \theta_1 \sin (\theta_1 + \theta_2))\varepsilon_1 \\ \quad + \Lambda \sin \theta_1 \sin \theta_2 \\ z_s = -\sin \theta_2 \sin (\theta_1 + \theta_2)\varepsilon_2 - \sin \theta_2 \cos (\theta_1 + \theta_2)\varepsilon_1 \\ \quad + \Lambda \cos \theta_2 \end{cases} \quad (10)$$

It is then possible to calculate roughly an altitude(θ_{2S}) and azimuth(θ_{1S}) for the Sun applying the Cartesian to spherical coordinates conversion (Eq. 5). This position is approximate and relative to the tracker since it does not take into account the Euler angles described in the last section, but what matters is the signs of the differences between these calculated values and the current altitude and azimuth relative to the tracker, defined by θ_1 and θ_2 . The angular corrections to apply on the two axes are then:

$$\begin{cases} d_{\theta 1} = \text{sgn}(\theta_{1S} - \theta_1)k_1 \\ d_{\theta 2} = \text{sgn}(\theta_{2S} - \theta_2)k_2 \end{cases} \quad (11)$$

Where k_1 and k_2 are the tracking angle steps that should be small to have a smooth tracking, yet large enough for the mechanical resolution of the rotation stages and the apparent movement of the Sun. The azimuth changes for instance at a rate of 15° per hour, assuming 1 second between the steps, k_1 should not be under 0.004° .

3 Application for a FTIR measurement station

Our group has been doing FTIR measurements at Reunion Island for several years ([22],[23],[24]). The place is interesting since atmospheric measurements are sparse in the tropical and subtropical region. Aiming at long-term monitoring and cost-effectiveness, a station at Saint-Denis (20.9°S , 55.5°E , 50m a.s.l.) has been automatized [25], which includes sun tracking, meteorological logging and FTIR measurements with a Bruker 120M. The solar tracker currently used is a commercial one from Denver University. Since September 2009, this station is officially part of the NDACC network. We plan to install a second FTIR on the Maïdo Observatory (21.1°S , 55.4°E , 2200 m a.s.l.) which will start operations in early 2012. This station, which will also be automatized, will be based on a Bruker 125 HR spectrometer, more appropriate to measure CO_2 atmospheric loading, in the framework of the new Total Carbon Column Observing Network (TCCON). The spectrometer is now tested at Brussels with an altazimuthal Sun tracker built at our institute, which was used to validate the methods described in the last section.

The new solar tracker uses a Newport RV-160 rotation stage for the azimuth rotation and a Vextra stepping motor with a gear box for the altitude. Both rotations are driven by a Newport XPS controller, linked to the controlling PC. The tracker mirrors are elliptical with a 10 cm minor axis. The photodiode set-up was purchased from Bruker with the spectrometer and is installed at the input window of the spectrometer. It consists of a 1 cm mirror which reflects a small portion of the incoming light to a 18 cm focal length lens which focuses the beam onto the 4-quadrant photodiode. The optical path is shown in Fig.6. The FOV of the 4-quadrant photodiode is 20 mrad (see Sect. 2.1). The algorithm used to compute the ephemeris is the one given by NOAA ([21]). During operation, the mirrors positions are refreshed every second according to the calculated position or to the signal on the 4-quadrant photodiode using the methods described in 2.3. From Fig.6, it is clear that the beam from the tracker undergo two rotations of

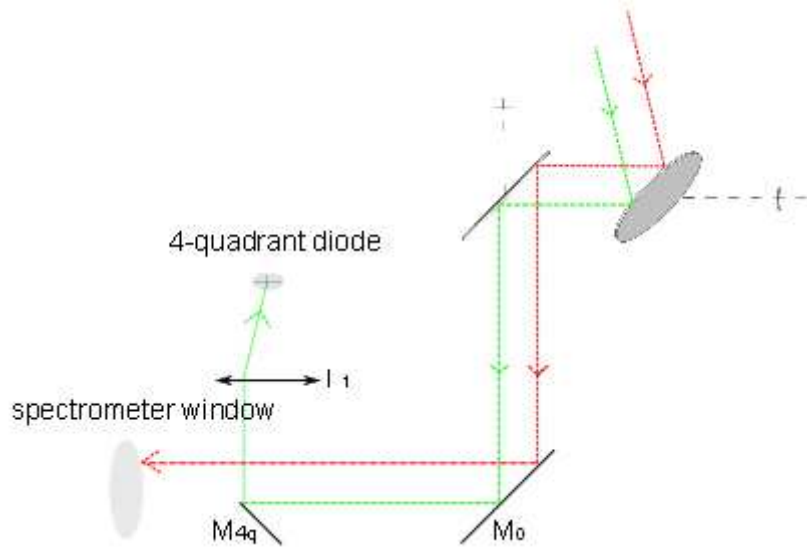


Figure 6: Optical paths of our particular set-up from the tracker to the spectrometer and the 4-quadrant diode.

90° along the same axis before hitting the photodiode, which we take into account inverting Eq. 11.

Figure 7 shows a fit of the Euler Angles. The track was performed on 8 February 2011 at BIRA-IASB in Brussels. The left panel shows the calculated mirror positions neglecting Euler Angles, together with the actual one when the active tracker was operational. Weather was clear-sky and enabled, despite the short winter daylight, to record a long Sun path, demonstrating the capacity of the active tracking algorithm described in Sect 2.3. Around one hundred points were extracted from the log file of the tracker position and used to fit the Euler Angles with a unconstrained non-linear minimization. The pitch, roll and yaw were respectively estimated to be -0.128° , -0.736° and -1.22° . The right panel shows how these fitted angles improve the calculated Sun position. The maximum offset between calculated and actual position is now 0.5° , i.e 9 mrad, which is under the 20 mrad of the photodiode's FOV. Providing this accuracy in the calculated mode, the tracking system is able to set the sun's image onto the 4-quadrant photodiode and then start the active tracking without the need of an operator.

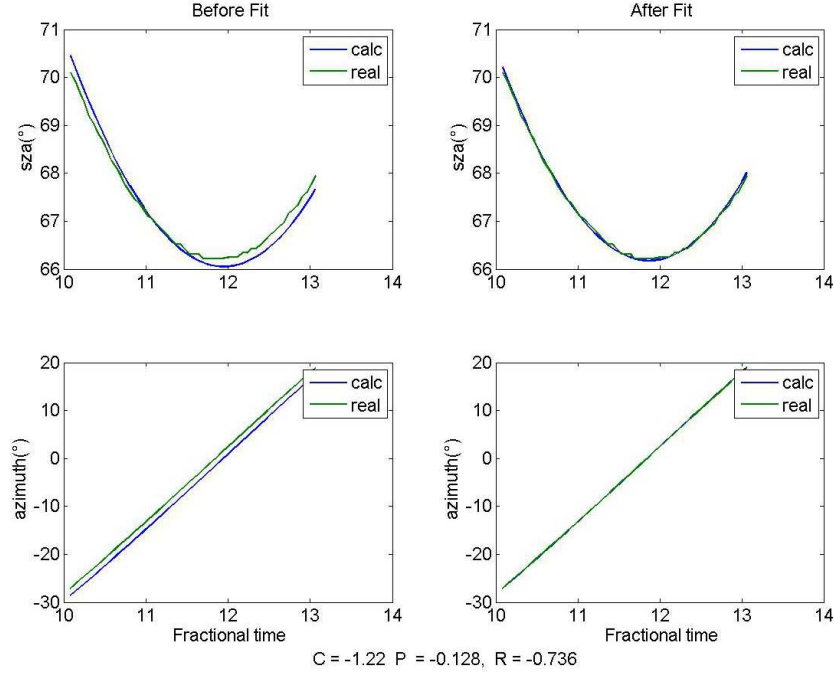


Figure 7: Fit of the Euler Angles.

4 Conclusion

We have derived the geometry formulas needed to track the Sun with a kind of altazimuthal tracker widely used in atmospheric remote sensing. The setup is based on two rotating 45° mirrors facing each other and a 4-quadrant photodiode involved in a closed-loop control of the tracker. After discussing the required accuracy for the calculated mode and calculating the FOV of the sensor, we described how to take into account and estimate the Euler angles, representing the orientation of the tracker compared to the ground. These sections can actually be applied to other tracking set-ups. On the other hand, even if the method is general, the formula for the active tracking depend strongly on the optical configuration and may not be used for other tracker's geometry. Finally, we have tested the formulas with a custom-built solar tracker that will be installed together with a FTIR spectrometer at Reunion Island in 2011.

The next steps involve the determination of the actual tracking accuracy with, for instance the Doppler shift of the Fraunhofer lines of the Sun. In case it is needed, the tracking smoothness could be improved with a PID control instead of the basic retroaction scheme presented here. Another improvement, which can not really worked out at our mid-latitude observatory in Brussels, would consist in finding a solution for the singularity occurring

at zenith. Indeed, when the solar zenith angle becomes too small, the azimuth has very little effect and the closed-loop tracking gets unstable. This is a common problem with altazimuthal system and leads to a dead measuring time of around one hour at local noon for the NDACC station already existing at Saint-Denis. We will deal with this problem if it is significant for our new tracker.

References

- [1] B. Barret, M. De Mazière, and P. Demoulin. Retrieval and characterization of ozone profiles from solar infrared spectra at the jungfraujoch. *Journal of Geophysical Research*, 107:15 PP., 2002.
- [2] M. De Mazière, C. Vigouroux, T. Gardiner, M. Coleman, P. Woods, K. Ellingsen, M. Gauss, I. Isaksen, T. Blumenstock, F. Hase, I. Kramer, C. Camy-peyret, P. Chelin, E. Mahieu, P. Demoulin, P. Duchatelet, J. Mellqvist, A. Strandberg, V. Velasco, J. Notholt, R. Sussmann, W. Stremme, and A. Rockmann. The exploitation of ground-based fourier transform infrared observations for the evaluation of tropospheric trends of greenhouse gases over europe. *Environmental Sciences*, 2:283–293, 2005.
- [3] M. Van Roozendael, P. Peeters, H. K Roscoe, H. De Backer, A. E Jones, L. Bartlett, G. Vaughan, F. Goutail, J. -P Pommereau, E. Kyro, C. Wahlstrom, G. Braathen, and P. C Simon. Validation of Ground-Based visible measurements of total ozone by comparison with dobson and brewer spectrophotometers. *Journal of Atmospheric Chemistry*, 29:55–83, 1998. 10.1023/A:1005815902581.
- [4] R. P. Cageao, J.-F. Blavier, J. P. McGuire, Y. Jiang, V. Nemtchinov, F. P. Mills, and S. P. Sander. High-Resolution Fourier-Transform Ultraviolet-Visible spectrometer for the measurement of atmospheric trace species: Application to OH. *Applied Optics*, 40(12):2024–2030, April 2001.
- [5] Shuhui Wang, Thomas J. Pongetti, Stanley P. Sander, Elena Spinei, George H. Mount, Alexander Cede, and Jay Herman. Direct sun measurements of NO₂ column abundances from table mountain, california: Intercomparison of low- and high-resolution spectrometers. *Journal of Geophysical Research*, 115:16 PP., July 2010.
- [6] E. Spinei and G.H. Mount. O₄ absorptions cross-section derived from direct sun measurements at different locations. *Manuscript in preparation*, 2011.

- [7] Galle B., Mellqvist J., Arlander D. W., Floisand I., Chipperfield M. P., and Lee A. M. Ground based FTIR measurements of stratospheric species from harestua, norway during sesame and comparison with models. *Journal of Atmospheric Chemistry*, 32:147–164, 1999.
- [8] M. Huster. Bau eines automatischen sonnenverfolgers fr bodengebundene ir-absorptionsmessungen. Master’s thesis, IMK, October 1998.
- [9] R. A. Washenfelter, G. C. Toon, J.-F. Blavier, Z. Yang, N. T. Allen, P. O. Wennberg, S. A. Vay, D. M. Matross, and B. C. Daube. Carbon dioxide column abundances at the wisconsin tall tower site. *Journal of Geophysical Research*, 111:11 PP., November 2006.
- [10] A. Merlaud. Development of a solar tracker for monitoring of atmospheric gases at harestua observatory. Technical report, May 2006.
- [11] A. Merlaud. Development of solar tracker for studies of volcanic gas emissions. Master’s thesis, ENSPG, September 2004.
- [12] A. Cordenier. Système numérique de régulation en position de miroirs destinés au suivi du rayonnement solaire. Master’s thesis, ECAM, 2004.
- [13] M. C. Geibel, C. Gerbig, and D. G. Feist. A new fully automated ftir system for total column measurements of greenhouse gases. *Atmospheric Measurement Techniques*, 3(5):1363–1375, 2010.
- [14] M. Gisi, F. Hase, S. Dohe, and T. Blumenstock. Camtracker: a new camera controlled high precision solar tracker system for ftir-spectrometers. *Atmospheric Measurement Techniques*, 4:47–54, 2011.
- [15] C.-W. Wong K.-K. Chong. General formula for on-axis sun-tracking system and its application in improving tracking accuracy of solar collector. *Solar Energy*, 83:298–305, 2009.
- [16] Kok-Keong Chong, Chee-Woon Wong, Fei-Lu Siaw, Tiong-Keat Yew, See-Seng Ng, Meng-Suan Liang, Yun-Seng Lim, and Sing-Liong Lau. Integration of an on-axis general sun-tracking formula in the algorithm of an open-loop sun-tracking system. *Sensors*, 9(10):7849–7865, 2009.
- [17] Jean Meeus. *Astronomical Algorithms*. Atlantic Books, December 1998.
- [18] Reda. Solar position algorithm for solar radiation applications. *Solar Energy*, 76(5):577–589.
- [19] V. Roy. sun_position.m. <http://www.mathworks.com/matlabcentral/fileexchange/4605-sunposition-m>, February 2009.
- [20] Philip E. Ciddor. Refractive index of air: new equations for the visible and near infrared. *Appl. Opt.*, 35(9):1566–1573, 1996.

- [21] General solar position calculations. <http://www.srrb.noaa.gov/highlights/sunrise/solareqns.PDF>
- [22] M. De Mazière, C. Vigouroux, P. F. Bernath, P. Baron, T. Blumenstock, C. Boone, C. Brogniez, V. Catoire, M. Coffey, P. Duchatelet, D. Griffith, J. Hannigan, Y. Kasai, I. Kramer, N. Jones, E. Mahieu, G. L. Manney, C. Piccolo, C. Randall, C. Robert, C. Senten, K. Strong, J. Taylor, C. Ttard, K. A. Walker, and S. Wood. Validation of ACE-FTS v2.2 methane profiles from the upper troposphere to the lower mesosphere. *Atmospheric Chemistry and Physics*, 8:2421–2435, 2008.
- [23] C. Senten, M. De Mazière, B. Dils, C. Hermans, M. Kruglanski, E. Neefs, F. Scolas, A. C. Vandaele, G. Vanhaelewyn, C. Vigouroux, M. Carleer, P. F. Coheur, S. Fally, B. Barret, J. L. Baray, R. Delmas, J. Leveau, J. M. Metzger, E. Mahieu, C. Boone, K. A. Walker, P. F. Bernath, and K. Strong. Technical note: New ground-based FTIR measurements at ile de la runion: observations, error analysis, and comparisons with independent data. *Atmos. Chem. Phys.*, 8:3483–3508, 2008.
- [24] C. Vigouroux, F. Hendrick, T. Stavrakou, B. Dils, I. De Smedt, C. Hermans, A. Merlaud, F. Scolas, C. Senten, G. Vanhaelewyn, S. Fally, M. Carleer, J.-M. Metzger, J.-F. Mller, M. Van Roozendael, and M. De Mazière. Ground-based ftir and max-doas observations of formaldehyde at runion island and comparisons with satellite and model data. *Atmospheric Chemistry and Physics*, 9(24):9523–9544, 2009.
- [25] E. Neefs, M. De Mazière, F. Scolas, C. Hermans, and T. Hawat. BARCOS, an automation and remote control system for atmospheric observations with a bruker interferometer. *Review of Scientific Instruments*, 78(3):035109, 2007.